

# Separation of Large-Diameter Metallic and Semiconducting Single-Walled Carbon Nanotubes by Iterative Temperature-Assisted Gel-Column Chromatography for Enhanced Device Applications

Sweejiang Yoo, Wenhui Yi,\* Asif Khalid, Jinhai Si, and Xun Hou

It is a challenging and application-oriented goal to achieve the metal/semiconductor separation of large diameter single-walled carbon nanotubes (SWCNTs) using a dextran-based gel chromatograph. Herein, a study of the temperature effect on the metal/semiconductor separation of plasma torch SWCNTs through dextran-based gel chromatograph is conducted. The temperature governs the interaction between SWCNTs and hydrogel, thus enabling the sorting of SWCNTs by electronic type. In addition, the temperature effect enables the metallic (m-) and semiconducting (sc-) fraction to be resolved and eluted using a single cosurfactant system, so that the process can be iterated easily. The fractions containing up to 99% of sc-SWCNTs and 95% of m-SWCNTs have been obtained after three times of iteration. The iteration process is not only applicable to sc-SWCNTs and m-SWCNTs, but also practicable for the cosurfactant system and circumvents additional preparation steps.

## 1. Introduction

Single-walled carbon nanotubes (SWCNTs) are analogous to a graphene layer wrapped-up into a seamless cylinder, where the wrapping vector is determined by a pair of integers (n,m).<sup>[1]</sup> The electrical properties of SWCNTs are heavily dependent on the (n,m) indices and the diameter of SWCNTs can be determined by applying the relationship,  $d_{\rm t}(n,m)=0.0783(n^2+m^2+nm)^{\frac{1}{2}}$ . The as-synthesized SWCNTs are in the complex mixture of many different SWCNTs or (n,m) species typically. Hence, the separation of SWCNTs according to the electronic type, diameter or (n,m) indices is vitally important to enhance the performance of SWCNTs in the integrated circuits,  $^{[2]}$  quantum light sources,  $^{[3]}$  sensors, and therapeutics. $^{[4]}$ 

Dr. S. Yoo, Dr. W. Yi, Dr. A. Khalid, Prof. J. Si, Prof. X. Hou Laboratory for Information Photonic Technology of ShaanXi Province & Key Laboratory for Physical Electronics and Devices of the Ministry of Education

School of Information and Electronics Engineering Xi'an Jiaotong University Shaanxi 710049, China

E-mail: yiwenhui@mail.xjtu.edu.cn

The ORCID identification number(s) for the author(s) of this article can be found under https://doi.org/10.1002/pssb.201900714.

DOI: 10.1002/pssb.201900714

goal, [5] the separation of SWCNTs is achieved by applying such techniques as density gradient ultracentrifuge, [6] aqueous two-phase extraction, [7] DNA-assisted separation, [8] selective polymer extraction, [9] and gel chromatography. The carrier mobility of SWCNTs is found out to scale quadratically with nanotubes diameter,[10] whereas exciton binding energy scales inversely with nanotubes diameter.[11] Therefore, the semiconducting SWCNTs with a large diameter (sc-SWCNTs, diameter  $(d_t)$ >1 nm) are preferable in high-performance computation for a large drive current.[12] In addition, the incorporation of sc-SWCNTs with a large diameter would improve the solar cells and infrared detectors due to their lower exciton binding energy and

As an important application-oriented

greater carrier mobility.[13]

Among various separation techniques, gel chromatography is a scalable technique for the separation of SWCNTs due to its simplicity, high throughput, and low cost. However, for gel chromatograph, the separation of SWCNTs with a large diameter is significantly more challenging than SWCNTs with a smaller diameter. The binding of SWCNTs to hydrogel can be described by a kinetically driven competitive binding model. [14] The affinity between nanotubes and hydrogel is governed by the differences in surfactant shell. The nanotubes with the strongest affinity bind first to the hydrogel, thus enabling their selective extraction according to electronic type. [14] However, SWCNTs with a large diameter have reduced difference in nanotubes' properties between species as the larger radius of curvature reduces the differentiation in the electronic structure and likely the differences in surfactant shell. Second, SWCNTs with a large diameter are covered with more surfactants or a larger surfactant shell due to stronger polarization (oxidation) caused by smaller bandgaps. The larger surfactant shell leads to weak retention forces in hydrogel, which inevitably complicates the separation.<sup>[15]</sup>

So far, gel chromatography has been optimized with sodium hydroxide (NaOH) tuning, temperature, iteration, and surfactant-composition gradient to realize electronic-typed separation of SWCNTs with a large diameter and high purities. [12b,15a,16] The NaOH optimization also enables the electronic-typed separation of double-walled carbon nanotubes with an outer wall diameter on the same order of SWCNTs with a large diameter.

www.pss-b.con

In this article, an investigation is conducted into the temperature effect on the metal/semiconductor separation of SWCNTs with a large diameter ( $d_{\rm t} > 1$  nm) by means of a dextran-based gel chromatograph. It is demonstrated that the purity of sc-SWCNTs and m-SWCNTs are improved at 30 and 40 °C, respectively. The absorbed SWCNTs are eluted at low temperature (12 °C). Therefore, the metallic and semiconducting fractions are resolved and eluted using a single cosurfactant system. As only a single cosurfactant system is applied, the process can be easily iterated by simply reloading the separated fraction into column again to achieve a higher purity. The fractions containing up to 99% of sc-SWCNTs and 95% of m-SWCNTs are obtained after three times of iteration.

## 2. Result and Discussion

#### 2.1. Metal/Semiconductor Separation

To separate SWCNTs, the temperature modulation was applied in sequence. First, the parent suspension ( $d_t = 0.9-1.5$  nm) was passed through a 5 mL Sephacryl-200 packed column preequilibrated at 25 °C. The unabsorbed SWCNTs were collected and set aside for separation at different temperatures. To elute the absorbed SWCNTs, the temperature was equilibrated at 12 °C. Subsequently, the eluent was applied (**Figure 1**). **Figure 2**a shows the optical absorption spectra of the eluted SWCNTs at different separation temperatures.  $S_{22}$  represents the  $E_{22}$  optical transition of sc-SWCNTs, whereas  $M_{11}$  indicates the  $E_{11}$  optical transition of m-SWCNTs. As shown in Figure 2a,b, as most SWCNTs species were selectively adsorbed by the hydrogel at 30, 35, and 40 °C, respectively, only an insignificant amount of SWCNTs were left at 45 and 50 °C (which would be discounted from discussion).

As shown in Figure 2c, SWCNTs separated at 30 °C show very strong  $S_{22}$  peaks and nearly vanishing  $M_{11}$  band, which indicates the enrichment of sc-SWCNTs. When the separation temperature increases to 35 °C, larger sc-SWCNTs are selectively enriched according to the strong and red-shifted  $S_{22}$  peaks. In comparison, the nanotubes sorted at 40 °C show intense  $M_{11}$  peaks and attenuated  $S_{22}$  peaks, suggesting the enrichment of m-SWCNTs. The metal/semiconductor separation as observed

can be attributable to the effect of temperature on the interaction difference between SWCNTs and hydrogel.[17] At 30 °C, only sc-SWCNTs with a smaller diameter show sufficient interaction with hydrogel to occupy the adsorption sites, whereas the unbound nanotubes, including sc-SWCNTs with a larger diameter and most m-SWCNTs flow through the gel. Among these unbound nanotubes, the larger sc-SWCNTs having sufficient interaction with hydrogel end up occupying the adsorption sites at 35 °C. Meanwhile, the unbound nanotubes, mostly m-SWCNTs in this case, flow through the hydrogel. The m-SWCNTs fraction ends up showing sufficient interaction with hydrogel to occupy the adsorption sites at 40 °C. A small amount (<1-5 wt%) of nanotubes is irreversibly adsorbed on the gel column in each separation run as discussed in Liu et al. works.[18] Despite the small number of irreversible nanotubes affords the gel column to be reused about three runs for the metal/semiconductor separation.<sup>[18a]</sup> We used a fresh gel column for the separation at 30, 35, and 40 °C, respectively. It avoids the changing of available adsorption sites due to irreversible adsorption from the previous run.

There is a possibility that increasing the temperature suppresses oxidation, thus leading to a lower density of surfactant and stronger interaction with hydrogel. The presence of H<sup>+</sup> and O<sup>2</sup> is known to make the oxidation (or protonation) of SWCNTs with a large diameter easier due to smaller bandgap. The reduction potential of O<sup>2</sup> and H<sup>+</sup>/H<sub>2</sub>O was reported to vary with temperature. [19] In addition. Liu and coworkers demonstrated that the temperature could affect the oxidation of different SWCNTs in sodium dodecyl sulfate (SDS) solution. Hence, a stepwise increase in temperature could lead to the successive adsorption of sc-SWCNTs in the order from smaller diameter to large diameter, and then the m-SWCNTs. Similarly, Yahya et al. proposed that the temperature could change the SDS micelles structure as well as coverage density on nanotube. [17b] The SDS micelles shrink in size and get loosely packed as the temperature increases. It then promotes the absorption of SWCNTs onto hydrogel due to weaker repulsion barrier from steric hindrance and electrostatic interaction.

Conversely, at low temperatures, the SDS micelles around the nanotubes experience structural rearrangement from parallel semicylindrical surface to herringbone pattern, which leads to

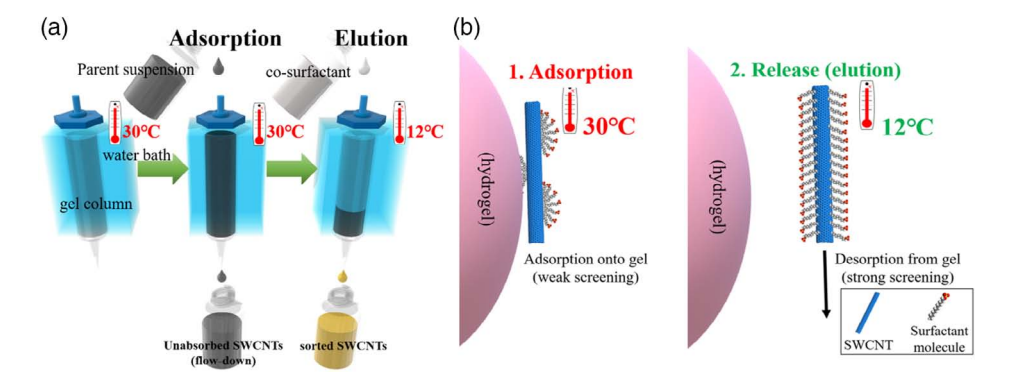


**Figure 1.** a) Illustration of the selective adsorption and elution of SWCNTs by temperature modulation. The adsorbed SWCNTs are eluted at low temperature (12 °C). b) A cartoon to illustrate the rearrangement of surfactant morphology and coverage density as the temperature changes. The surfactant coverage density increases and the molecules convert to herringbone pattern as the temperature reaches 12 °C. Eventually, the SWCNTs will desorb from the adsorption sites (hydrogel) due to the strong screening effect. The SWCNTs then move through the column as elution fraction.

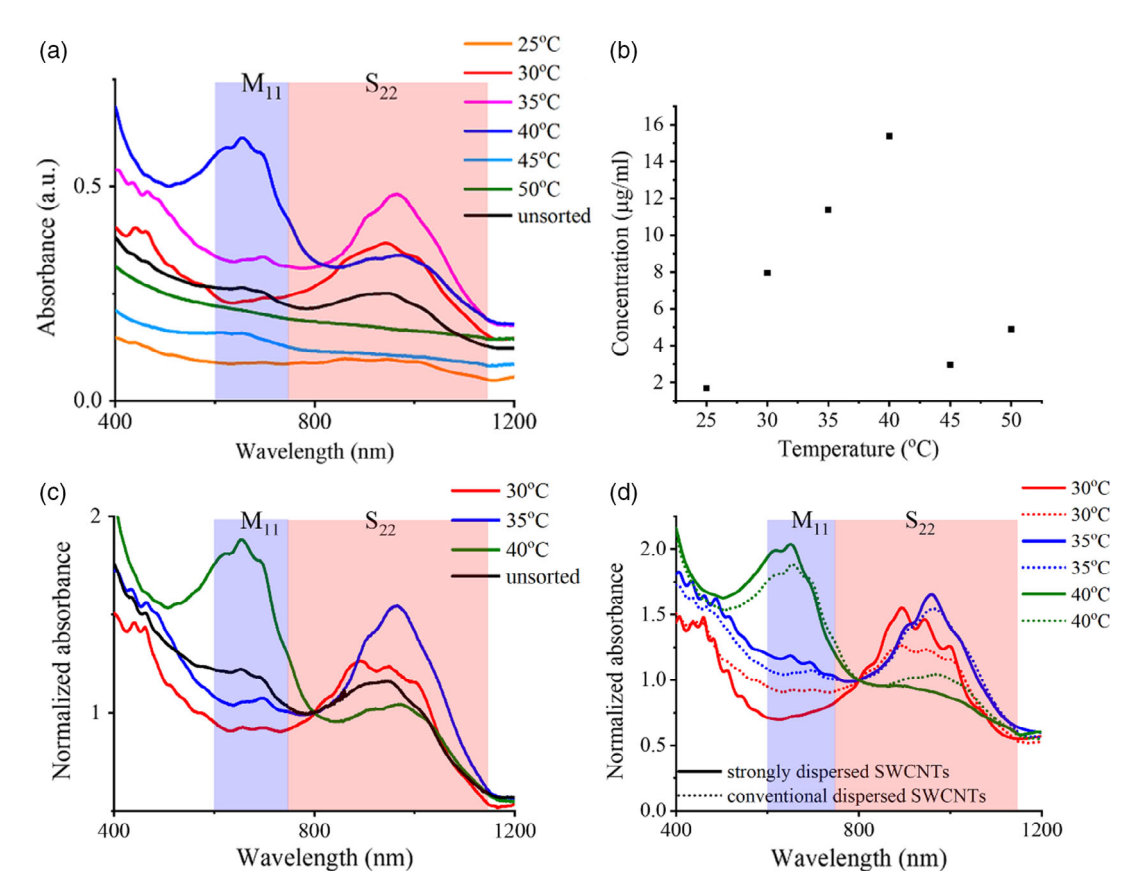


Figure 2. a,b) The UV-vis-NIR spectra at different separation temperatures and their concentrations. c) The UV-vis-NIR spectra for separation temperatures at 30, 35, and 40 °C. d) The UV-vis spectra (strongly dispersed SWCNTs and conventional-dispersed SWCNTs) for separation temperatures at 30, 35, and 40 °C.

an increment in coverage density. [5,20] As a result, the SWCNTs are eluted or flow through the hydrogel due to repulsion barrier overcoming the van der Waals interaction. Similarly, the micellization of sodium cholate (SC) is affected by the temperature. The SC mean aggregation number typically decreases as the temperature increases, despite the relatively small changes in aggregation number. [21] Considering the Krafft point for SDS and SC ( $\approx$ 14 and 17 °C, respectively) and the crystallization temperature for SDS ( $\approx$ 8 °C), 12 °C is chosen for elution to avoid the possible SDS crystallization (e.g.,  $\approx$ 8 °C@ 2 wt%). [22]

In addition, the zeta potential of sc-SWCNTs was measured at different temperatures (**Figure 3b**). The linear relationship between zeta potential and temperature indicates that the lower temperature stabilizes the nanotubes against van der Waals interaction better. The reason is supposed to be related to the changes of surfactant coverage density and orientation on nanotube in function of temperature. To demonstrate how the temperature and nanotube diameter affects the surfactant coverage density, another separation was conducted by loading the parent suspension at 30 °C. Then, the temperature was gradually reduced by 2.5 °C. The optical spectra (Figure 3a) reveal that the  $S_{22}$  peaks experience a monotonic blue shift as the temperature decreases from 30 to 10 °C, for which the desorption of SWCNTs follows the diameter sequence. In fact, SWCNTs with

a larger diameter could be oxidized more easily compared with SWCNTs with a smaller diameter due to the presence of a smaller bandgap. They tend to be covered with surfactants, as a result of which they would be eluted earlier as temperature declines.

## 2.2. Iteration

As demonstrated by previous studies, iterative separation improves the outcome of metal/semiconductor separation. However, the elution of adsorbed SWCNTs is usually achieved by changing the eluent and introducing salt or acidic aqueous. It makes iteration difficult as they are hard to remove and return to the initial eluent. As inspired by Tulevski et al., [12b] the separation is iterated easily if the separated fraction is resolved and eluted using a single surfactant system. Herein, the absorbed SWCNTs are eluted at low temperature (12 °C). Therefore, the metallic and semiconducting fractions are resolved and eluted using a single cosurfactant system. Then, the separation was iterated by simply reloading the separated fraction into column again to achieve a higher electronic purity. The separation for each temperature (30, 35, and 40 °C) was iterated three times. To better illustrate the iterative effect, two parent suspensions were prepared under





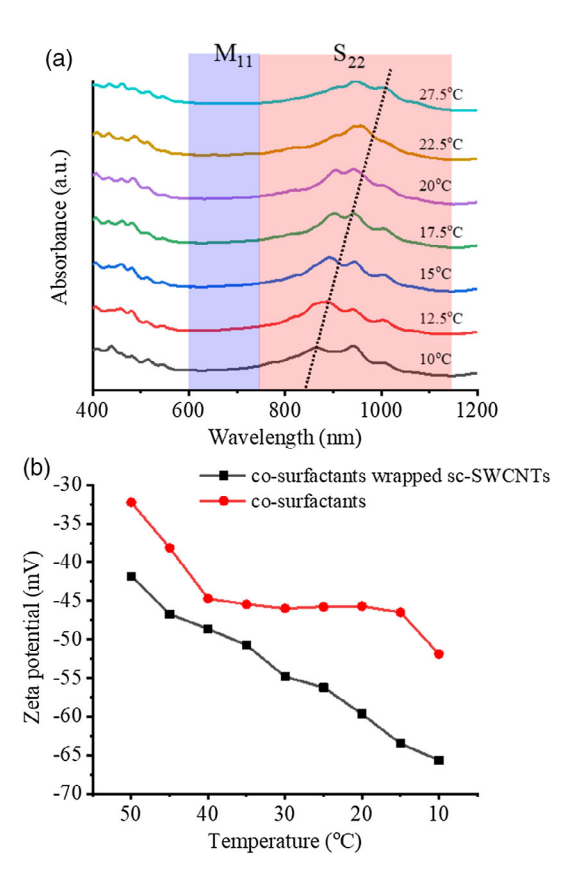


**Figure 3.** a) The optical absorption spectra of the eluted SWCNTs at different temperatures (from 27.5 to  $10\,^{\circ}$ C) in stepwise manner. b) Zeta potential of cosurfactant-wrapped sc-SWCNTs (red) and cosurfactant (black) in the function of temperature.

different sonication conditions: 1) conventionally dispersed SWCNTs (0.5 wt% SDS @ 120 W for 1 h). 2) strongly dispersed SWCNTs (2 wt% SDS @ 200 W for 3.5 h). Figure 2d shows the optical absorption spectra of the strongly dispersed SWCNTs and conventional-dispersed SWCNTs at different separation temperatures. According to previous reports, the absorption peak ratio  $(\phi_i)$  was calculated to quantitatively indicate the degree of separation and considered as the designated metric to describe the sc-purity. [24]  $\phi_i$  is defined as  $A_{CNT}/(A_{CNT}+A_B)$ , where  $A_{CNT}$ indicates the area enveloped by  $M_{11}$  and  $S_{22}$  peaks with linear baseline subtraction, and A<sub>B</sub> denotes the area below the same region. [24,25] Typically, the  $\phi_{\rm i}$  values over 0.08, 0.31, and 0.33 correspond to >70%, 95%, and 99% sc-purity, respectively.[24] As  $\phi_i$  value is incapable to reveal the m-purity, a simple optical evaluation method was applied to estimate the metallic-tosemiconducting ratio for SWCNTs m-purity(%) =  $\left(\frac{1}{1+1.24\frac{\lambda}{9}}\right)$ . Unlike  $\phi_i$  value, the general model directly estimates the m-purity as a percentage. [26]

To begin with, the first iteration is examined. On the basis of Figure 2d, the  $\phi_i$  values are calculated to be 0.3 and 0.18 for strongly dispersed SWCNTs sorted at 30 and 35 °C, suggesting the sc-purity of 70–95%, respectively, whereas those are 0.22 and 0.22 for conventional-dispersed SWCNTs. In contrast, the m-purity is calculated to be 88% and 65% for strongly dispersed

SWCNTs and conventionally dispersed SWCNTs sorted at 40 °C, respectively. As shown in **Figure 4**a, upon each iteration, the  $S_{22}$ peaks are made stronger and narrower, whereas the  $M_{11}$  bands are suppressed, indicating a significant sc-purity enhancement after each iteration. The calculated  $\phi_i$  values for strongly dispersed SWCNTs sorted at 30 °C are 0.3, 0.37, and 0.37 for the first, second, and third iterations, respectively, whereas those for conventionally dispersed SWCNTs are 0.22, 0.29, and 0.34. Therefore, the sc-purity reaches 99% after three iterations. It is also noticed that conventional-dispersed SWCNTs have a much lower  $\phi_i$  value after the first iteration but considerable increments after the second and third iterations, which is in contrast with strongly dispersed SWCNTs. This could be accounted for by the difference preparation conditions of the parent suspensions, which could affect the interaction strength difference between m-SWCNTs-hydrogel and sc-SWCNTshydrogel.<sup>[27]</sup> Conventional-dispersed SWCNTs with shorter sonication time have a less significant interaction strength difference, thus leading to lower sc-purity and requiring more iterations to reach the same sc-purity.

Resembling trend (Figure 4b) is observed for the iterative sorting at 35 °C. The calculated  $\phi_i$  values for strongly dispersed SWCNTs are 0.18, 0.24, and 0.24 after the first, second, and third iterations, respectively, whereas those for conventionaldispersed SWCNTs are 0.22, 0.23, and 0.26. The sc-purity is estimated to be 70–95%. [24,28] It is noticeable that the metal/ semiconductor separation at 35 °C is poorer than at 30 °C, which is primarily attributed to the subtle interaction strength difference between sc-SWCNTs with a larger diameter-hydrogel and m-SWCNTs-hydrogel. For iterative sorting at 40 °C (Figure 4c), the calculated m-purity for strongly dispersed SWCNTs are 88%, 92%, and 95% after the first, second, and third iterations, whereas those are 65%, 84%, and 84% for conventionaldispersed SWCNTs. The iteration was further examined (strongly dispersed SWCNTs) with Raman spectroscopy under 633 and 733 nm excitation. The radial breathing mode (RBM) peaks stemming from m-SWCNTs and sc-SWCNTs are shown in Figure 4e,f. After being sorted at 30 °C (under 633 nm excitation), the G<sup>-</sup> band and G<sup>+</sup> band show a Lorentzian line shape, and a typical sign for sc-SWCNTs further confirms the absence of m-SWCNTs. After being sorted at 35 °C for three times of iteration, the G- band exhibits a broader Breit-Wigner Fano (BWF) line shape, indicating the presence of m-SWCNTs. This is excellently consistent with the relatively low  $\phi_i$  values and low sc-purity on the basis of the optical absorption analysis as mentioned in the previous section. After being sorted at 40 °C for three times of iteration, the G band exhibits an asymmetric BWF line shape, whereas the RBM peaks of sc-SWCNTs are further attenuated, thus confirming the enrichment of m-SWCNTs. This confirms to the aforementioned optical absorption analysis. Under 785 nm excitation, after being sorted at 30 °C, the RBM peaks from m-SWCNTs fail to be detected after multiple iterations, which suggest high sc-purity. After being sorted at 35 °C, the metallic peaks remain observed after iterations, which is consistent with the broader BWF line shape on G band mentioned earlier. This further confirms the low sc-purity. After being sorted at 40 °C for three times of iteration, the RBM peaks stemming from m-SWCNTs are detected, whereas the RBM peaks of sc-SWCNTs are further attenuated, which evidences

15213951, 2020, 5, Downloaded from https://onlinelibrary.wiley.com/doi/10.1002/pssb.201900714 by CAS-XIAN INSTITUTION OPTICS PRECISION MECHANICS, Wiley Online Library on [10/11/2025]. See the Terms

nditions) on Wiley Online Library for rules of use; OA articles are governed by the applicable Creative Commons License

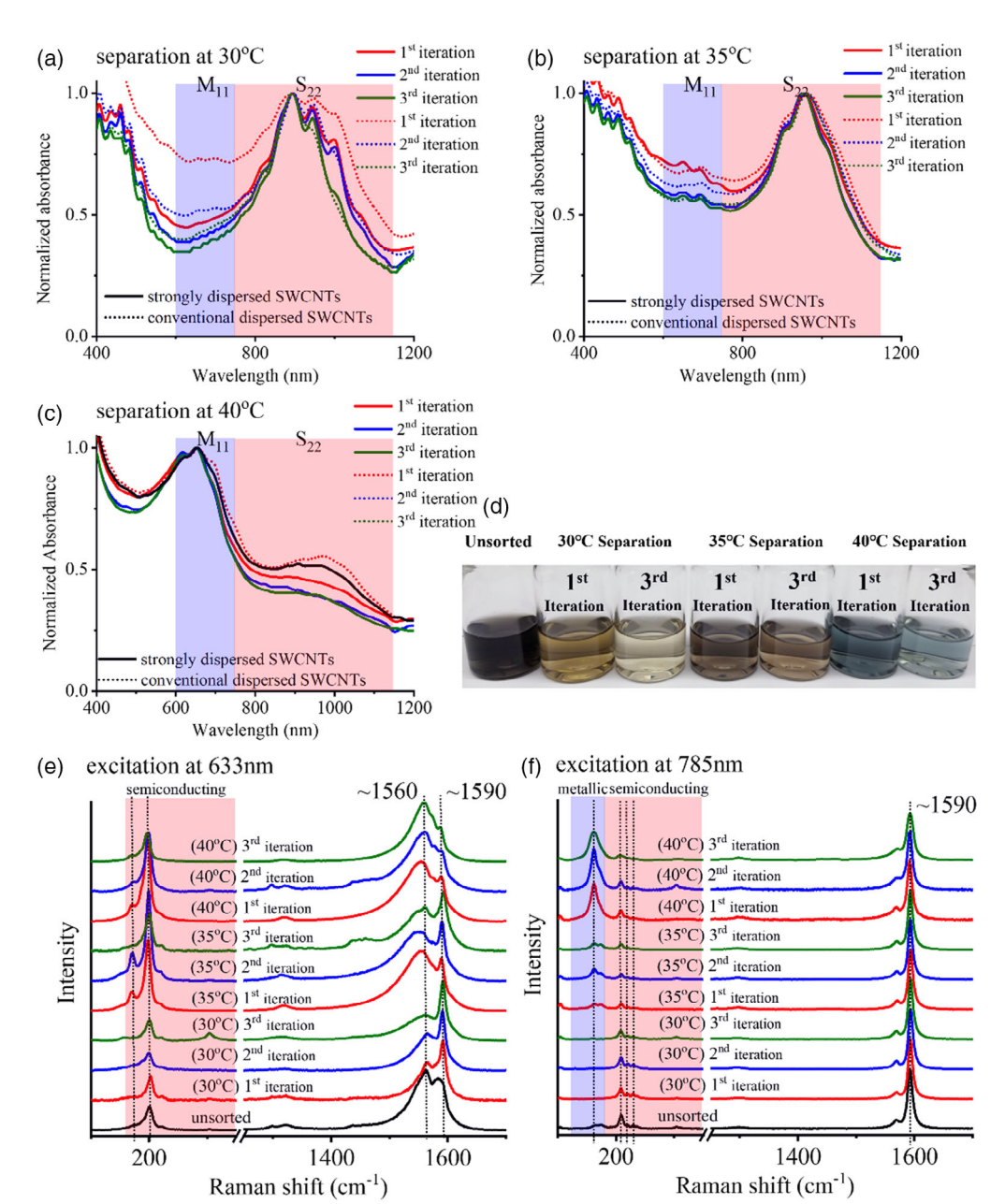


Figure 4. The UV-vis-NIR spectra for iterations at different separation temperatures a) 30 °C, b) 35 °C, and c) 40 °C. All the UV-vis-NIR spectra were normalized to 800 nm for ease of comparison and clarity. d) Photograph of separated SWCNTs (strongly dispersed SWCNTs). e,f) The Raman spectra (strongly dispersed SWCNTs) for separation at 30, 35, and 40 °C under 633 and 785 nm excitation. All Raman spectra were normalized to the G-band at ≈1590 cm<sup>-1</sup> and offset for clarity. The RBM signals of SWCNTs are heavily dependent on the nanotube's diameter.

the enrichment of m-SWCNTs. The iteration improves the purity of both sc-SWCNTs and m-SWCNTs.

### 3. Conclusions

In summary, we report the metal/semiconductor separation of large-diameter SWCNTs using temperature-assisted gel chromatograph. The temperature effect also allows the separated fraction to be resolved and eluted using a single cosurfactant system, thus simplifying the iteration process. The sc-purity and m-purity reach  $\approx$ 99% and 95%, respectively, after three times of iteration. As plasma-torch SWCNTs and gel chromatograph have the advantages of low cost, our findings could be used in the low-cost production of high-mobility sc-SWCNTs and m-SWCNTs inks.

## 4. Experimental Section

Materials and Methods: Plasma-torch SWCNTs (RN-220) were purchased from Raymor Industries Inc. The Sephacryl S-200HR

physi

www.advancedsciencenews.com

(GE Healthcare), SDS (Acros  $\geq$ 99%), and SC (TCI  $\geq$ 98%) were used directly without any further purification.

Dispersion: 1) conventional-dispersed SWNCTs: A 100 mg of RN - 220 SWCNTs powder was suspended in 100 mL aqueous 0.5 wt% SDS by tip sonication (Scientz-IID, 120 W) for 1 h while being immersed in a water bath (12 °C). The dispersion was centrifuged at 2 15 000  $\times$  g (Sorvall WX100) for 1 h to sediment out amorphous carbon and large bundles. About 80 mL of supernatant was mixed with 1 wt% SDS/1 wt% SC solution to obtain 160 mL 0.75 wt% SDS/0.5 wt% SC dispersion. 2) strongly dispersed SWNCTs. About 100 mg portion of RN-220 SWCNTs powder was suspended in 100 mL aqueous 2 wt% SDS by tip sonication (Scientz-IID, 200 W) for 3.5 h while immersed in a water bath (12 °C). The dispersion was centrifuged at 2 15 000  $\times$  g (Sorvall WX100) for 1 h to sediment out amorphous carbon and large bundles. About 40 mL of supernatant was diluted by 40 mL deionized water. Then, the diluted supernatant was mixed with 0.5 wt% SDS/1 wt% SC solution to obtain 160 mL 0.75 wt% SDS/0.5 wt% SC dispersion.

Metal/Semiconductor Separation of SWCNTs: Conventional-dispersed SWCNTs were considered as parent suspension. Then, a 5 mL separation column was filled with Sephacryl S-200 as filtration medium. To investigate the effect of temperature, the metal/semiconductor separation was conducted at different temperatures (25-50 °C) in sequence. Hence, the parent suspension, SDS/SC solution (0.75 wt% SDS/0.5 wt% SC), and gel column were immersed in a water bath (Scientz DC-3010). To perform separation, the temperature of water bath was pre-equilibrated at 25  $^{\circ}\text{C}$  for 15 min. The separation column was then flushed with SDS/SC solution using a peristaltic pump (Longer BT100, ≈10 rpm). Then, 160 mL of parent suspension was applied to the separation column. The flow-through fraction was collected and set aside for the next-time separation (as the parent suspension for subsequent temperature separation). Subsequently, 20 mL of SDS/SC solution was applied to elute the unbound SWCNTs. The adsorbed SWCNTs were collected by equilibrating the temperature to only 12 °C for 15 min. Finally, SDS/SC solution was applied to elute the adsorbed SWCNTs. The separation experiments were conducted at six different temperatures, which include 25, 30, 35, 40, 45, and 50 °C. To investigate how the temperature affects the surfactant coverage density in diameter manner, another metal/semiconductor separation was performed by loading the parent suspension at 30 °C. Then, the temperature was equilibrated at 27.5 °C for 15 min. SDS/SC solution was applied to elute the adsorbed SWCNTs. The experiment procedures were repeated from 27.5 to  $10\,^{\circ}\text{C}$  in stepwise.

Iteration: The prepared parent suspensions (conventional-dispersed SWCNTs and strongly dispersed SWCNTs) were used. The experiment procedures were the same as mentioned earlier (metal/separation of SWCNTs) except that each temperature separation was repeated three

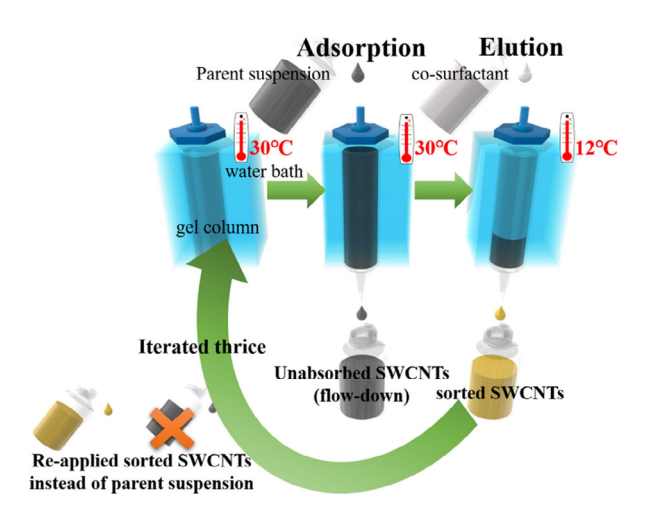


Figure 5. Illustration of iterative process at 30 °C.

times (30, 35, and 40 °C). The iteration was performed by reloading the separated fraction into the separation column again at the same temperature (**Figure 5**). However, there was a slight modification made to temperature separation at 40 °C. For 40 °C separation, the parent suspension (flow-through fraction from 35 °C) was applied to column, and the adsorbed fraction was collected at 12 °C, which then completed the first iteration. To start second iteration, the adsorbed fraction from previous iteration was applied. However, the flow-through fraction was collected, and the eluted fraction 12 °C was discarded. It then completed the second iteration, which was repeated twice.

Characterization: Optical absorbance spectra were measured using an ultraviolet—near-infrared spectrophotometer (LAMDA 950, Perkin Elmer). Raman spectra for 633 and 785 nm excitation were measured using a confocal Raman microscope (HR800, Horiba). The zeta potentials were obtained using Zetasizer Nano zs90.

# Acknowledgements

The authors thank Miss Wang and Miss Lu at the Instrument Analysis Center of Xi'an Jiaotong University for their assistance with Raman and optical absorbance spectra measurement. This research was generously supported by the National Key R & D Program of China (grant nos. 2019YFA0706400 and 2019YFA0706402), Natural Science Foundation of China (nos. 61275179 and 60970815), the Natural Science Basic Research Plan in Shaanxi Province of China (program no. 2016JM8047), the Fundamental Funds for the Central Universities (no. xjj2015112), and ShaanXi Province Administration of Traditional Chinese Medicine (15-ZY036).

### **Conflict of Interest**

The authors declare no conflict of interest.

#### **Keywords**

gel chromatography, iterative sorting, large diameter single-walled carbon nanotubes, nanotube separation, temperature effect

Received: November 12, 2019 Revised: December 31, 2019 Published online: January 22, 2020

- J. W. Wilder, L. C. Venema, A. G. Rinzler, R. E. Smalley, C. Dekker, Nature 1998, 391, 59.
- [2] a) D. Zhong, Z. Zhang, L. Ding, J. Han, M. Xiao, J. Si, L. Xu, C. Qiu, L.-M. Peng, Nat. Electron. 2018, 1, 40; b) J. Tang, Q. Cao, G. Tulevski, K. A. Jenkins, L. Nela, D. B. Farmer, S.-J. Han, Nat. Electron. 2018, 1, 191.
- [3] a) X. He, H. Htoon, S. Doorn, W. Pernice, F. Pyatkov, R. Krupke, A. Jeantet, Y. Chassagneux, C. Voisin, Nat. Mater. 2019, 18, 770;
  b) X. He, N. F. Hartmann, X. Ma, Y. Kim, R. Ihly, J. L. Blackburn, W. Gao, J. Kono, Y. Yomogida, A. Hirano, Nat. Photonics 2017, 11, 577;
  c) A. Graf, C. Murawski, Y. Zakharko, J. Zaumseil, M. C. Gather, Adv. Mater. 2018, 30, 1706711.
- [4] a) C. Zhu, A. Chortos, Y. Wang, R. Pfattner, T. Lei, A. C. Hinckley, I. Pochorovski, X. Yan, J. W.-F. To, J. Y. Oh, Nat. Electron. 2018, 1, 183; b) A. L. Antaris, J. T. Robinson, O. K. Yaghi, G. Hong, S. Diao, R. Luong, H. Dai, ACS Nano 2013, 7, 3644; c) Y. Yomogida, T. Tanaka, M. Zhang, M. Yudasaka, X. Wei, H. Kataura, Nat. Commun. 2016, 7, 12056; d) S. Diao, G. Hong, J. T. Robinson, L. Jiao, A. L. Antaris, J. Z. Wu, C. L. Choi, H. Dai,



- J. Am. Chem. Soc. 2012, 134, 16971; e) T. Murakami, H. Nakatsuji, M. Inada, Y. Matoba, T. Umeyama, M. Tsujimoto, S. Isoda, M. Hashida, H. Imahori, J. Am. Chem. Soc. 2012, 134, 17862.
- [5] B. S. Flavel, M. M. Kappes, R. Krupke, F. Hennrich, ACS Nano 2013, 7, 3557.
- [6] M. S. Arnold, A. A. Green, J. F. Hulvat, S. I. Stupp, M. C. Hersam, Nat. Nanotechnol. 2006, 1, 60.
- [7] J. A. Fagan, E. H. Hároz, R. Ihly, H. Gui, J. L. Blackburn, J. R. Simpson, S. Lam, A. R. Hight Walker, S. K. Doorn, M. Zheng, ACS Nano 2015, 9,
- [8] M. Zheng, A. Jagota, M. S. Strano, A. P. Santos, P. Barone, S. G. Chou, B. A. Diner, M. S. Dresselhaus, R. S. Mclean, G. B. Onoa, Science 2003, 302, 1545.
- [9] a) H. W. Lee, Y. Yoon, S. Park, J. H. Oh, S. Hong, L. S. Liyanage, H. Wang, S. Morishita, N. Patil, Y. J. Park, Nat. Commun. 2011, 2, 541; b) S. Park, H. W. Lee, H. Wang, S. Selvarasah, M. R. Dokmeci, Y. J. Park, S. N. Cha, J. M. Kim, Z. Bao, ACS Nano 2012, 6, 2487.
- [10] X. Zhou, J. Y. Park, S. Huang, J. Liu, P. L. Mceuen, Phys. Rev. Lett. **2005**, 95, 146805.
- [11] R. B. Capaz, C. D. Spataru, S. Ismail-Beigi, S. G. Louie, Phys. Status Solidi B 2010, 244, 5.
- [12] a) Z. Chen, J. Appenzeller, J. Knoch, Y. M. Lin, P. Avouris, Nano Lett. 2005, 5, 1497; b) G. S. Tulevski, A. D. Franklin, A. Afzali, ACS Nano **2013**, 7, 2971.
- [13] a) Y. Liu, N. Wei, Q. Zhao, D. Zhang, S. Wang, L.-M. Peng, Nanoscale 2015, 7, 6805; b) Y. Liu, N. Wei, Q. Zeng, J. Han, H. Huang, D. Zhong, F. Wang, L. Ding, J. Xia, H. Xu, Adv. Opt. Mater. 2016, 4, 238.
- [14] K. Tvrdy, R. M. Jain, R. Han, A. J. Hilmer, T. P. Mcnicholas, M. S. Strano, ACS Nano 2013, 7, 1779.
- [15] a) B. S. Flavel, K. E. Moore, M. Pfohl, M. M. Kappes, F. Hennrich, ACS Nano 2014, 8, 1817; b) D. Yang, J. Hu, H. Liu, S. Li, W. Su, Q. Li,

- N. Zhou, Y. Wang, W. Zhou, S. Xie, Adv. Funct. Mater. 2017, 27, 1700278.
- [16] a) Y. Miyata, K. Shiozawa, Y. Asada, Y. Ohno, R. Kitaura, T. Mizutani, H. Shinohara, Nano Res. 2011, 4, 963; b) B. Thendie, H. Omachi, J. Hirotani, Y. Ohno, Y. Miyata, H. Shinohara, Jpn. J. Appl. Phys. **2017**. *56*. 065102.
- [17] a) H. Liu, T. Tanaka, Y. Urabe, H. Kataura, Nano Lett. 2013, 13, 1996; b) I. Yahya, F. Bonaccorso, S. K. Clowes, A. C. Ferrari, S. R. P. Silva, Carbon 2015, 93, 574.
- [18] a) H. Liu, T. Tanaka, H. Kataura, Phys. Status Solidi (b) 2011, 248. 2524; b) H. Liu, D. Nishide, T. Tanaka, H. Kataura, Nat. Commun. **2011**, 2, 309.
- [19] A. Nish, R. J. Nicholas, Phys. Chem. Chem. Phys. 2006, 8, 3547.
- [20] C. A. Silvera-Batista, D. C. Scott, S. M. McLeod, K. J. Ziegler, J. Phys. Chem. C 2011, 115, 9361.
- [21] H. Sugioka, K. Matsuoka, Y. Moroi, J. Colloid Interface Sci. 2003, 259,
- [22] S. Paula, W. Sues, J. Tuchtenhagen, A. Blume, J. Phys. Chem. 1995, 99, 11742
- [23] L. Jiang, L. Gao, J. Sun, J. Colloid Interface Sci. 2003, 260, 89.
- [24] J. Ding, Z. Li, J. Lefebvre, F. Cheng, G. Dubey, S. Zou, P. Finnie, A. Hrdina, L. Scoles, G. P. Lopinski, Nanoscale 2014, 6, 2328.
- [25] a) M.-H. Lee, S.-H. Lee, J. Kim, S. Y. Lee, D.-H. Lim, K. Hwang, H. Hwang, Y. C. Jung, Y.-Y. Noh, D.-Y. Kim, Carbon 2017, 125, 571; b) K. S. Mistry, B. A. Larsen, J. L. Blackburn, ACS Nano 2013,
- [26] a) L. Huang, H. Zhang, B. Wu, Y. Liu, D. Wei, J. Chen, Y. Xue, G. Yu, H. Kajiura, Y. Li, J. Phys. Chem. C 2010, 114, 12095; b) Y. Miyata, K. Yanagi, Y. Maniwa, H. Kataura, J. Phys. Chem. C 2008, 112, 13187.
- [27] R. M. Jain, K. Tvrdy, R. Han, Z. Ulissi, M. S. Strano, ACS Nano 2014, 8, 3367.
- [28] J. Ouyang, J. Ding, J. Lefebvre, Z. Li, C. Guo, A. J. Kell, P. R. L. Malenfant, ACS Nano 2018, 12, 1910.